Specific Binding of CO to Tetraheme Cytochrome c_3[†]

Yuki Takayama,[‡] Yukiko Kobayashi,[‡] Naoki Yahata,[‡] Takashi Saitoh,[‡] Hiroshi Hori,[§] Takahisa Ikegami,[‡] and Hideo Akutsu*,[‡]

Institute for Protein Research, Osaka University, Yamadaoka, Suita 565-0871, Japan, and Graduate School of Engineering Science, Osaka University, Toyonaka 560-8531, Japan

Received September 13, 2005; Revised Manuscript Received January 20, 2006

ABSTRACT: Carbon monoxide (CO) has been identified as another bioactive molecule like NO. Binding of CO to a tetraheme cytochrome c_3 (cyt c_3) was investigated using visible absorption spectroscopy, circular dichroism (CD), and NMR. CO was found to bind to the four hemes in different manners. CD spectra, however, indicated that only single-site CO binding can keep the protein intact. The K_d for the single-site binding was 8.0 μM, which is a typical value for a CO sensor protein. Furthermore, NMR spectra of uniformly ^{15}N-labeled and specifically [^{15}N]His-labeled proteins have provided evidence that CO specifically binds to the sixth coordination site of heme 2 via single-site binding. The CO-bound cyt c_3 could conduct redox reactions. In light of triheme cytochrome c_7, the CO-bound cyt c_3 may work as an electron transporter. It was reported for sulfate-reducing bacteria that CO can be used as an energy source and CO cycling is operating like H_2 cycling. Therefore, the CO-bound cyt c_3 may play a role in maintaining electron transport pathways on accumulation of toxic CO for its utilization.

Cytochrome c_3 (cyt c_3)[1] is a small tetraheme protein mainly found in sulfate-reducing bacteria of the genus *Desulfovibrio* (*1*). This protein is classified as a class III *c*-type cytochrome (*2*). Each heme is covalently linked to two cysteine residues in a -C-X-X-C-H- or -C-X-X-X-X-C-H- sequence (X is any amino acid residue). A series of three-dimensional structures of cyt c_3 have been reported (*3* and references therein). The fifth and sixth ligands of the four hemes are all histidyl imidazoles. One of the remarkable features of this protein is the extremely low redox potential of the four hemes in comparison with other *c*-type cytochromes. The microscopic redox potentials of cyt c_3 from *Desulfovibrio vulgaris* Miyazaki F (*Dv*MF) have been estimated with the combined use of NMR and electrochemistry to be in the range of −265 to −370 mV versus the SHE (standard hydrogen electrode) (*4*, *5*). Heme−heme interactions strongly affect the redox potentials of each heme. This protein functions as an important electron transport protein in sulfate respiration (*1*). The physiological partners of cyt c_3 in sulfate respiration are believed to be [Fe]- and [NiFe]hydrogenases (*1*).

Carbon monoxide (CO) was reported to bind to cyt c_3 (*6*, *7*). CO has been well-known to strongly bind to five-coordinated ferrous heme in a protein and to inhibit its biological function. Since all hemes in cyt c_3 are hexacoordinated, the CO binding is unusual. On the other hand, it has been indicated recently that CO can work as a bioactive molecule to induce specific functions of heme proteins just as in the case of NO (*8*−*10*). Actually, *D. vulgaris* cells also can grow on CO (*11*) as photosynthetic bacteria that have a CO sensor protein CooA (*10*). CO cycling is operating in *D. vulgaris* in connection with its energy transduction (*11*). Therefore, binding of CO to cyt c_3 is particularly interesting. Since the nature of this binding has not yet been clarified, we have investigated its nature, using UV−visible absorption, circular dichroism (CD), and nuclear magnetic resonance (NMR) spectroscopy, and differential pulse polarography. The assignments of the coordinated imidazole NH signals as well as the amide signals of *Dv*MF cyt c_3 reported by us (*3*) were used for detailed characterization. Our results have revealed that a CO molecule specifically binds to the sixth coordination site of heme 2 via single-site binding, and cyt c_3 is a putative CO sensor protein regulating the electron transfer pathways.

MATERIALS AND METHODS

*Growth and Purification. Dv*MF cyt c_3 was expressed in *Shewanella oneidensis* TSP-C that had been transformed by the plasmid with the cloned gene, as described previously (*12*, *13*). The transformant was microaerobically grown at 30 °C. Three kinds of ^{15}N-labeled cyt c_3 were prepared, viz., uniformly ^{15}N-labeled, [1-^{15}N]His-labeled, and [U-^{15}N]His-labeled cyt c_3. Uniformly ^{15}N-labeled cyt c_3 was produced as described previously (*14*). [1-^{15}N]His-labeled cyt c_3 and [U-^{15}N]His-labeled cyt c_3 were obtained by growing the cells on a medium comprising 0.5 mM $CaCl_2$, 1.0 mM $MgSO_4$, 5.7 mM ammonium sulfate [$(NH_4)_2SO_4$], 5.7 mM K_2HPO_4, 3.3 mM KH_2PO_4, 2.0 mM $NaHCO_3$, 100 mM sodium succinate, and 140 mM Tris-HCl (pH 7.6) with an amino acid mixture and additional supplements. The supplements

[†] This research was partly supported by grants from the Ministry of Education, Science, Technology, Sport and Culture of Japan (Grant-in-Aid for Scientific Research on Priority Areas and CREST).

* To whom correspondence should be addressed: Institute for Protein Research, Osaka University, Yamadaoka, Suita 565-0871, Japan. E-mail: akutsu@protein.osaka-u.ac.jp. Phone: +81-6-6879-8597. Fax: +81-6-6879-8599.

[‡] Institute for Protein Research, Osaka University.

[§] Graduate School of Engineering Science, Osaka University.

[1] Abbreviations: cyt c_3, cytochrome c_3; *Dv*MF, *Desulfovibrio vulgaris* Miyazaki F; *Dv*H, *D. vulgaris* Hildenborough; CO, carbon monoxide; NMR, nuclear magnetic resonance; CD, circular dichroism; NaP_i, sodium phosphate.

10.1021/bi051867i CCC: $33.50
Published on Web 02/17/2006

included 0.1 g/L yeast extract, 56.6 μM HBO_3, 67.2 μM Na_2-EDTA, 1.26 μM $MnSO_4$, 1.04 μM $ZnSO_4$, 0.2 μM $CuSO_4$, 3.87 μM Na_2MoO_4, 5.4 μM $FeSO_4$, 5.0 μM $CoSO_4$, 5.0 μM $Ni(NH_4)_2(SO_4)_2$, 20 mg/L thiamine hydrochloride, α-biotin, adenosine, guanosine, cytidine, thymidine, and uridine at the given final concentrations. The amino acid mixture (all per liter of culture) consisted of 500 mg of Ala, 400 mg of Arg, 400 mg of Asn, 400 mg of Asp, 50 mg of Cys, 400 mg of Gln, 1 g of Glu, 550 mg of Gly, 300 mg of Ile, 400 mg of Leu, 450 mg of Lys, 100 mg of Met, 200 mg of Phe, 400 mg of Pro, 300 mg of Ser, 230 mg of Thr, 100 mg of Trp, 400 mg of Tyr, 300 mg of Val, and 150 mg of [1-^{15}N]- or [U-^{13}C,^{15}N]His (99% ^{15}N, Cambridge Isotope Laboratories, Inc.). Cyt c_3 was purified as follows. Harvested cells were suspended in 30 mM sodium phosphate (NaP_i) buffer (pH 7.0) with 0.1 mM 4-(2-aminoethyl)benzenesulfonyl fluoride hydrochloride and a small amount of deoxyribonuclease I and were sonicated using an Ultrasonic UD201 Disruptor (TOMY). After cellular debris had been removed, $(NH_4)_2SO_4$ was dissolved at 70% saturation. The suspension was centrifuged at 70000*g* for 30 min. The supernatant was loaded onto a Phenyl-Sepharose 26/10 column (Amersham Bioscience) equilibrated with 70% saturated $(NH_4)_2SO_4$ in 30 mM NaP_i buffer (pH 7.0) and developed with a 70 to 0% gradient of saturated $(NH_4)_2SO_4$ in 30 mM NaP_i buffer (pH 7.0). The cyt c_3 fractions were collected and dialyzed against 30 mM NaP_i buffer (pH 7.0). They were loaded onto a SP-Sepharose 26/10 column (Amersham Bioscience) equilibrated with 30 mM NaP_i buffer (pH 7.0) and eluted with a 0 to 400 mM NaCl gradient in 30 mM NaP_i buffer (pH 7.0). Cyt c_3 fractions were collected, dialyzed against ultrapure water, and then lyophilized. The purity was checked by SDS−polyacrylamide gel electrophoresis. $^{15}NH_4Cl$ (99% ^{15}N) and ^{13}CO gas (99% ^{13}C) were purchased from Shokotsusho Ltd. [NiFe]Hydrogenase was purified from *Dv*MF as reported in a previous paper (*13*).

CO Titrations. CO titration of ferrous cyt c_3 was performed in 100 mM NaP_i buffer (pH 7.0) at 25 °C under anaerobic conditions. A cyt c_3 solution (1−4 μM protein) was placed in a cuvette covered with a rubber septum. Cyt c_3 was reduced by a sufficient amount of sodium dithionite dissolved in the same buffer. For CO titration, aliquots of CO-saturated 100 mM NaP_i buffer including sodium dithionite were added to the cyt c_3 solution. After incubation at 25 °C for 10 min, absorption spectra were recorded with a Beckman DU640 spectrometer, which was controlled at 25 °C.

Circular Dichroism (CD) Measurements. CD spectra for far-UV (190−270 nm), near-UV (270−390 nm), and Soret band (390−440 nm) regions were obtained using 4 μM cyt c_3 [30 mM NaP_i buffer (pH 7.0)] in a 1 mm path length quartz cell. For measurement of the amount of CO-bound cyt c_3, the sample was fully reduced by flushing H_2 gas in the presence of 4 nM [NiFe]hydrogenase, and then aliquots of CO-saturated 30 mM NaP_i buffer were added to the cyt c_3 solution. After incubation at 25 °C for 10 min, CD spectra were measured with a Jasco J-720WI CD spectropolarimeter. UV−visible absorption spectra were recorded before and after each CD measurement to confirm that there is no change during the measurement. A solvent spectrum measured under the same conditions was subtracted to obtain the actual sample spectrum. The results are expressed in terms of mean residue ellipticity.

NMR Measurements. Samples containing 0.5 mM cyt c_3 in 100 mM NaP_i buffer (90% H_2O and 10% ^2H_2O) at pH 7.0 were prepared as described previously (*5*). After cyt c_3 was reduced by sodium dithionite powder, a N_2/CO (3:1) gas mixture was flushed onto the surface of the sample solution. When the protein concentration was as high as 1 mM, aggregation was observed. After the NMR measurements, the pH of each sample solution was confirmed. Heteronuclear NMR spectra were recorded at 30 °C on AVANCE DRX-500 and DRX-600 NMR spectrometers (Bruker). ^{1}H−^{15}N HSQC spectra of complete and amide regions were acquired with 2048 × 512 and 2048 × 256 points, which were zero-filled to 4096 × 1024 and 4096 × 512 points, respectively. The spectral width was 21 ppm with a carrier frequency of 4.7 ppm for ^{1}H and 70 and 40 ppm with carrier frequencies of 135 and 120 ppm for ^{15}N of complete and amide regions, respectively. A three-dimensional NOESY ^{1}H−^{15}N HSQC spectrum was measured with 2048 (^{1}H) × 128 (^{1}H) × 16 (^{15}N) points and a mixing time of 100 ms in the fully reduced state. The spectrum was zero-filled to 4096 × 256 × 32 points with spectral widths of 21, 14, and 70 ppm, respectively. A ^{13}C NMR spectrum of ^{13}CO-bound cyt c_3 was measured at 30 °C and 100.6 MHz with an AV-400M spectrometer (Bruker). The spectral width and number of points were 100 ppm and 16 384, respectively. Chemical shifts are presented in parts per million relative to 2,2-dimethyl-2-silapentane-5-sulfonate (DSS) as an internal reference.

Electrochemical Measurements. Differential pulse polarograms were recorded at 30 °C under anaerobic conditions with a PerkinElmer 394 digital electrochemical trace analysis system, using a dropping mercury electrode and an Ag/AgCl reference electrode. The modulation amplitude, sweep rate, and drop time were 20 mV, 2 mV/s, and 2 s, respectively. The protein concentration was 0.1 mM in 30 mM NaP_i buffer (pH 7.0). For measurement of the amount of CO-bound cyt c_3, the protein was fully reduced by the flushing of H_2 gas in the presence of [NiFe]hydrogenase, followed by the flushing of CO gas onto the surface of the reduced solution just before every measurement. The potential was scanned from −500 to 300 mV. The redox potentials are referenced to the standard hydrogen electrode (SHE).

RESULTS

CO Titration. The visible absorption spectrum of fully reduced cyt c_3 on CO titration is presented in Figure 1A. Reduced cyt c_3 gives absorption bands at 552, 523, and 418 nm, which are replaced by those at 564, 534, and 413 nm, respectively, which are typical for an absorption spectrum of a CO-bound heme (*7*, *15*). The spectral changes on CO titration gave isosbestic points, showing a transition between two spectral forms. Since the final CO concentration gave rise to a typical spectrum of the CO-bound heme, CO should bind to every heme of cyt c_3 at this CO concentration. Taking this into account, we plotted the level of formation of CO-bound heme as a function of CO concentration in Figure 1B. The reproducibility of the titration curve for 1.3 μM cyt c_3 was confirmed as shown in the figure. Clearly, there are multiple titration curves overlapping each other with retardations in CO concentration. Especially, a typical saturation curve was observed for the first binding up to 60 μM. A similar titration curve was obtained for 3.3 μM cyt c_3, except

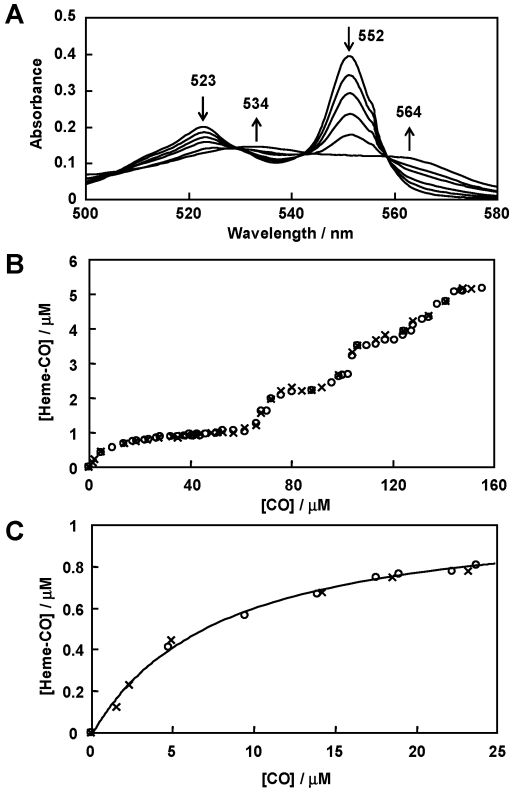

FIGURE 1: CO titration of fully reduced cytochrome c_3 at pH 7.0 and 25 °C. (A) Visible absorption spectra in the presence of 0, 28, 75, 113, 142, and 377 μM CO. Typical peaks are indicated with wavelength (nanometers). The arrows show the direction of the spectral changes with an increase in CO concentration. (B) Amount of CO-bound heme as a function of CO concentration. The CO-bound heme concentration was calculated from the absorbance change at 552 nm. Circles and crosses represent two independent experimental data. (C) Experimental data in panel B were fitted with the equation $[CO] = [heme{\cdot}CO](K_d + [C_O] - [heme{\cdot}CO])/([C_O] - [heme{\cdot}CO])$, where [CO], $[C_O]$, and [heme·CO] are the concentrations of total CO, total protein, and CO-bound heme, respectively. The solid line is the best-fit curve. The concentration of cyt c_3 was 3.3 μM for panel A and 1.3 μM for panels B and C. The absorption spectra did not change for 2 h.

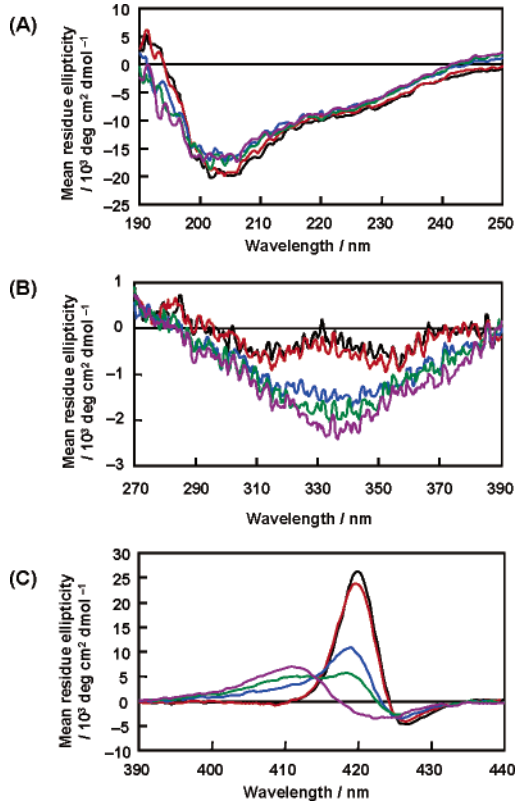

FIGURE 2: Circular dichroism spectra of fully reduced cytochrome c_3 in the absence (black) and in the presence of 40.9 (red), 81.8 (blue), 122.7 (green), and 188.7 μM (purple) CO in far-UV (A), near-UV (B), and Soret band (C) regions.

that the second CO binding started at ~42 μM CO. O'Connor et al. (*7*) suggested via time-resolved absorption and magnetic circular dichroism (MCD) that CO bound to the four hemes of cyt c_3 as sixth ligands. This is consistent with our results in panels A and B of Figure 1.

To examine the effect of binding of CO on cyt c_3 structure, circular dichroism (CD) spectra were measured at 40.9, 81.8, 122.7, and 188.7 μM CO. They correspond to one, two, three, and more CO bindings to cyt c_3 on average, respectively, judging from Figure 1B. Since the visible spectra before and after CD measurements were identical (spectra were not shown), the state of the cyt c_3 solution did not change during CD measurements. There were no significant changes in the spectra in three wavelength regions for the fully reduced and single CO-bound cyt c_3 (0 and 40.9 μM, respectively) as can be seen in Figure 2. When the CO concentration was 81.8 μM, however, the secondary structure content was slightly reduced judging from the far-UV CD spectra (Figure 2A). The tertiary structure was also affected in light of the near-UV CD spectra (Figure 2B). The spectrum in the Soret band region changed significantly (Figure 2C), suggesting a change in the heme architecture. Now, it can be concluded that while the single CO-bound cyt c_3 keeps its structure almost intact, binding of more CO molecules changes its structure, including the heme architecture. Therefore, the binding data at low CO concentrations (up to 25 μM) were analyzed using a model for 1:1 complex formation (Figure 1C). The obtained K_d value was 8.0 ± 0.2 μM. In contrast to CO, O_2 oxidizes the reduced cyt c_3 only without binding. NO also did not bind to it. Therefore, cyt c_3 specifically binds CO. Since the second CO binding takes place cooperatively, depending on CO and CO-bound cyt c_3 concentrations, it would involve oligomerization of the proteins. We have tried to identify the CO binding site in cyt c_3 by NMR measurements.

Effect of CO Binding on $^1H-^{15}N$ HSQC Spectra of Cytochrome c_3. $^1H-^{15}N$ HSQC spectra of uniformly ^{15}N-labeled and specifically [1-^{15}N]His-labeled cyt c_3 were measured in the fully reduced state. All cross-peaks have been assigned previously (*3*). Taking advantage of the assignments, we examined the effect of CO binding. N_2/CO (3:1, 0.5 mL) gas was flushed onto the surface of the sample solution, resulting in ~12.5% CO in the gas phase above the sample solution. The CO concentration in water should be 47 μM in equilibrium. The imidazole imide region of a $^1H-^{15}N$ HSQC spectrum of uniformly ^{15}N-labeled cyt c_3 is presented in Figure 3A. Eight cross-peaks represent those in the fully reduced state. The noncoordinated imidazole of His67 did not give rise to a signal because of fast exchange. The cross-peaks in the presence of CO are presented in Figure 3B. Seven cross-peaks have newly appeared (colored red) in addition to the original ones, showing the coexistence of multiple molecular species. Since the newly apparent

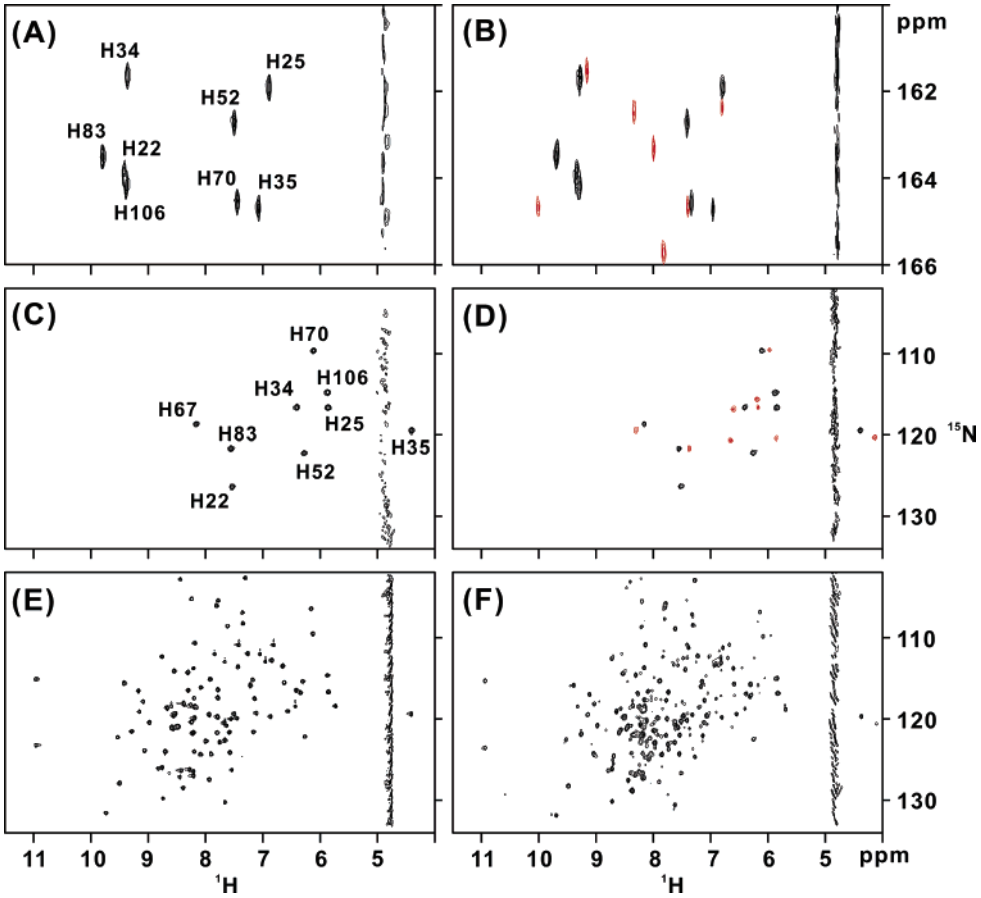

FIGURE 3: $^{1}H-^{15}N$ HSQC spectra of fully reduced cytochrome c_3 in the absence (A, C, and E) and presence (B, D, and F) of CO at pH 6.9 and 30 °C. (A and B) Imide signals and (E and F) amide signals of uniformly ^{15}N-labeled cyt c_3 measured at 600 MHz with a spectral width of 70 ppm. (C and D) Amide signals of [1-^{15}N]His-labeled cyt c_3 at 500 MHz with a spectral width of 40 ppm. Newly apparent signals are colored red in panels B and D. His34, His52, His83, and His106 are fifth axial ligands and His22, His35, His25, and His70 sixth axial ligands of hemes 1−4, respectively.

cross-peaks are different from those in the three-electron-reduced state (S_3), they can be assigned to the coordinated imidazoles of CO-bound cyt c_3. The binding of CO was directly confirmed by a ^{13}C NMR spectrum of ^{13}CO-bound cyt c_3, which revealed a broad signal at 208 ppm (spectrum not shown). This can be ascribed to the signals of ^{13}CO bound to a heme iron in light of the reported chemical shifts (∼208 ppm from DSS) for hemoglobins (*16*) and cytochrome *c* hemopeptide (*17*). As a result, we can conclude that CO actually binds to cyt c_3 and changes its structure.

Then, the CO concentration in aqueous solution was changed. The volume intensities of seven new signals revealed the same increase in rate with the increase in CO concentration, suggesting that they originate from a single species. The average volume intensity of new signals is plotted as a function of the expected CO concentration in Figure S1 of the Supporting Information. Although CO-bound cyt c_3 increases linearly with CO concentration, its amount is much smaller than that expected from Figure 1B. This should be ascribed to a slow diffusion of CO in viscous solution because of a high protein concentration, which resulted in the formation of a concentration gradient of CO along the sample tube axis with the expected concentration in the top region. Since the ratio of CO-bound to total cyt c_3 is much less than 1, only a single CO should be bound to cyt c_3 in light of Figure 1B. Now, it is most likely that CO binds to a specific single site, thereby inducing an overall conformational change (specific single-site binding model). A shift would occur for every signal but one, since the signal of the imidazole released from the coordination site by CO must disappear due to the fast exchange. This explains the appearance of seven new signals. However, the possibility that there are multiple CO-bound species, namely, cyt c_3 with CO bound at different sites (multiple-binding model), cannot be eliminated, and these K_d values were accidentally the same. There could be at most seven kinds of CO-bound cyt c_3 species according to the appearance of seven new signals.

The $^{1}H-^{15}N$ HSQC spectra of the fully reduced and CO-flushed [1-^{15}N]His-cyt c_3 solutions are presented in panels C and D of Figure 3, respectively. Nine cross-peaks were observed for all histidine residues (colored black, eight coordinated and one noncoordinated) in the fully reduced state. They were all assigned as shown in Figure 3C (*3*). There were 18 cross-peaks in the presence of CO due to nine new cross-peaks (colored red). Most of the new ones are located in the vicinity of the original ones, showing that every original signal has a single shifted counterpart. The simplest interpretation is that newly apparent signals come from a newly formed CO-bound cyt c_3. This is completely consistent with the specific single-site binding model mentioned above. When there are *n* CO-binding species (multiple-binding model), there should be at least $n + 7$ signals of axial His in Figure 3D because *n* imide signals of released His residues would be missing in Figure 3B. Here, it is

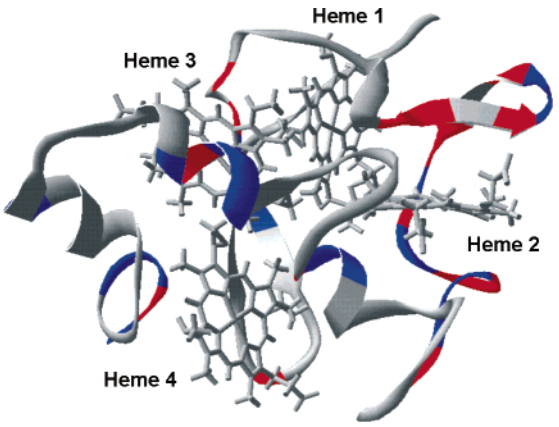

FIGURE 4: Residues showing large CO-induced perturbations mapped on the reduced cytochrome c_3 structure (*3*). For red portions, $\{[(\delta^1H)^2 + (\delta^{15}N/5)^2]/2\}^{1/2} > 0.15$, and for blue portions, $0.15 \geq \{[(\delta^1H)^2 + (\delta^{15}N/5)^2]/2\}^{1/2} > 0.10$ for the chemical shifts in the $^1H-^{15}N$ HSQC spectrum (Figure 3F). This figure was prepared with Swiss-PdbViewer (*25*).

assumed that when the chemical shift of an imidazole signal changes, that of the amide signal in the same residue also changes. This is likely in light of the structural strain of the coordinated residue. Only $n = 1$ satisfies the observed number, eight, suggesting that the multiple-binding model is inappropriate. To make the mode of binding more conclusive, the $^1H-^{15}N$ HSQC spectra, including all the amide signals, were also examined in the absence and presence of CO and presented in panels E and F of Figure 3, respectively. The new signals in the presence of CO are not colored this time because there are too many signals. Although the relationship between the original and newly apparent cross-peaks is not as straightforward as in panels B and D of Figure 3 due to the many signals, the number of the latter is clearly smaller than the number of the former. The residues showing great chemical shift perturbations are mapped onto the reduced solution structure in Figure 4. Significant changes were found in the region surrounding heme 2, suggesting that it constitutes the perturbed site. Most red-colored sites on the left in Figure 4 are His residues coordinated to hemes 1, 3, and 4. This observation also strongly supports the model in which the CO-bound cyt c_3 is just one species, and the CO binding affects a broad area of the protein. Taking the results given above in their entirety, we can conclude that CO binds to a single coordination site of cyt c_3, despite the fact that there are eight possible sites. This model is consistent with the observation in CD experiments that only single CO-bound cyt c_3 is intact from the structural point of view. The possible binding site is heme 2.

Identification of a CO-Binding Site. If one refers to Figure 3B, three of the seven new cross-peaks are found in the vicinity of the His25, His34, and His70 cross-peaks. It follows that these signals can be assigned to His25, His34, and His70 of CO-bound cyt c_3, respectively. This means that the fifth coordination site of heme 1 (His34) and the sixth coordination sites of hemes 3 (His25) and 4 (His70) are not occupied by CO, since they would disappear upon replacement with CO. When a heme-coordinated imidazole is substituted with CO, the coordination structure of the imidazole on the opposite side of the porphyrin ring will also change, resulting in a large shift of the imidazole cross-

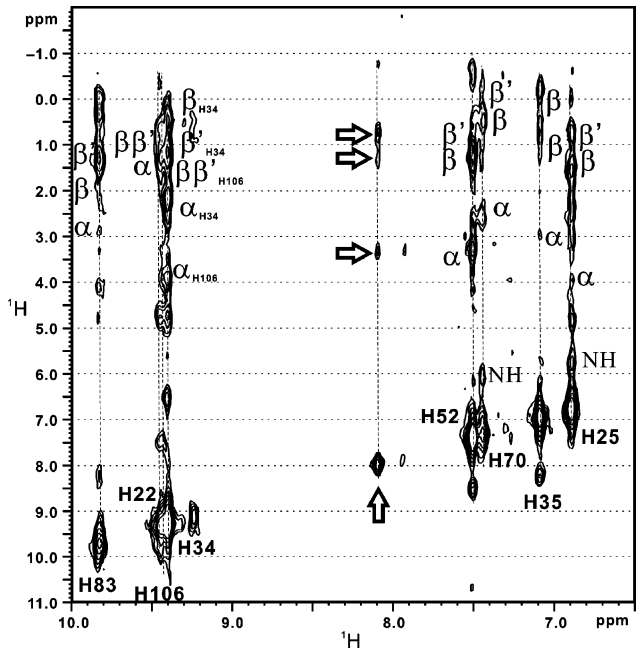

FIGURE 5: Two-dimensional section of three-dimensional NOESY $^1H-^{15}N$ HSQC spectrum of [U-^{15}N]His-labeled ferrous cytochrome c_3 in the presence of CO at a ^{15}N chemical shift of 163.2 ppm (the imide signal region). This spectrum was acquired at 600 MHz at pH 6.9 and 30 °C. The digital resolution in the ^{15}N dimension was 4.4 ppm. Imide cross-peaks are indicated by the corresponding His sequence number. The signals of interest are highlighted with arrows. The assignment for the NOE cross-peaks is also given in the figure. The letters α and β denote αCH and βCH_2 of an amino acid residue, respectively. When two protons of the latter are nonequivalent, β and β' are used for them.

peak. Since the chemical shift changes of the His25, His34, and His70 signals on CO binding are small, it is strongly suggested that the other coordination sites of hemes 3, 1, and 4 are not replaced with CO. Thus, it can be concluded that the CO-binding site is heme 2, in agreement with the chemical shift perturbation data mapped in Figure 4.

In a $^1H-^{15}N$ HSQC spectrum of partially oxidized cyt c_3 in the presence of CO, a cross-peak at 8.07 ppm remained unaffected whereas other peaks experienced changes in intensity (Figure S2 of the Supporting Information). This strongly suggests that the trans position of this imidazole is the CO-binding site. To assign this signal, a three-dimensional NOESY $^1H-^{15}N$ HSQC spectrum was measured using [U-^{15}N]His-labeled cyt c_3. A two-dimensional NOESY section of the imidazole NH part is presented in Figure 5. Since the digital resolution for the ^{15}N dimension was 4.4 ppm, this section covered all imide signals. The sharp signals at 8.07 and 9.24 ppm among the CO-bound signals gave cross-peaks. However, only the signal at 8.07 ppm gave clear NOE cross-peaks at 3.27, 1.39, and 0.79 ppm. Although a conformational change takes place on CO binding, changes in chemical shift would not be very large in light of the results in Figure 3F. Thus, we used the NOE cross-peaks to assign the signal. Since all α and β,β' hydrogens of the coordinated histidine residues are assigned (BioMagResBank entry 5333), we can compare the cross-peaks accurately despite the apparently low resolution of the spectrum. For example, the chemical shifts of αH and β,β'H are 3.01, 0.21, and −0.16 ppm and 3.28, 1.40, and 1.16 ppm for His35 (sixth ligand of heme 2) and His52 (fifth ligand of heme 2),

respectively. Taking the chemical shift change upon CO binding (Figure 3F) into account, we found only His52 data matched the observed values. This is also the case with other histidine residues, as seen in Figure 5. Thus, we assign this signal to His52 of CO-bound cyt c_3, indicating that the CO-binding site is the sixth coordination site of heme 2. This is consistent with the MCD result which shows that CO binds to the sixth coordination site of each heme (*7*).

In light of the agreement of three pieces of independent evidence mentioned above, we can conclude that CO binds to heme 2, specifically to its sixth coordination site. Upon partial oxidation of the reduced cyt c_3, the existence of the single CO-bound cyt c_3 in a partially oxidized state (S_3) was confirmed in the $^1H-^{15}N$ HSQC spectra of imides (Figure S2 of the Supporting Information). This indicated that the single CO-bound cyt c_3 could work as an electron transporter. When the sample solution is fully oxidized, the NMR spectrum reverts to that of fully oxidized cyt c_3 without any indication of CO binding. Therefore, the CO binding is reversible under the specific single-site binding conditions.

Measurement of Differential Pulse Polarograms. A differential pulse polarogram (DPP) of the CO-bound cyt c_3 was measured. At the first stage of CO flushing, the polarograms disappeared. When the color of the sample solution has changed because of CO binding, a new pattern started to appear. The polarograms comprised two reproducible peaks, a small one at −293 mV and a large one at 130 mV. This process suggests that in the first stage, CO binds to the mercury electrode since they are soft base and metal, respectively. Thus, the intact cyt c_3 could not give rise to a polarogram. This is also the case with the single CO-bound cyt c_3 because there is no peak in the low-potential region even during the color change. Then, the non-native protein might have started to compete with CO in binding to the electrode. The adsorbed protein would have given rise to the polarogram. Although a direct electron transfer could not be observed, the intact and single CO-bound cyt c_3 behaved in similar way in this experiment, suggesting that both have stable structures, in agreement with CD results. In contrast, more than one CO-bound cyt c_3 is apt to denature on the electrode as in the NMR sample solution.

DISCUSSION

It was shown in this work that CO binds to the sixth coordination site of heme 2 of cyt c_3 upon specific single-site binding and its structure is almost intact (Figure 2). The specific binding indicates that the coordination bond from His35 imidazole to the heme 2 iron is weak. In fact, the $N_\epsilon 2-Fe$ bonds of His35 and His52 are among the longest found in this protein (*13*). The weak coordination may be associated with the torsion angle of the two axial imidazole planes. It is about 64° at heme 2, while those at other hemes are less than 10° (*13*). CO also can bind to the other hemes as shown in Figure 1B, which is consistent with the report by O'Connor et al. (*7*) that CO binds to sixth coordination sites of the four hemes. Furthermore, they observed four first-order kinetic constants of 5.7, 62, 425, and 2900 μs for CO recombination with the heme iron after photodissociation (*7*). This suggests that the affinity of CO binding is significantly different for each heme. This is in good agreement with the CO binding isotherm in Figure 1B. In light of our CD experiment (Figure 2), however, cyt c_3 with more than one CO bound takes on a non-native structure. This would be the reason an NMR sample solution became aggregated at a high CO concentration. Namely, the non-native structure is soluble at a low cyt c_3 concentration but becomes insoluble when it is aggregated at a high concentration. Thus, we have seen only one species in the NMR spectra. In light of its intact structure, cyt c_3 with a single CO bound at the sixth coordination site of heme 2 might be still biologically active.

Heme 2 is unique in light of the structure of triheme cytochrome c_7 (cyt c_7). Cyt c_7 has a heme architecture similar to that of cyt c_3 but lacks heme 2 (*18*). Therefore, the architecture of active hemes in CO-bound cyt c_3 is similar to that of cyt c_7, and the surface charges should be similar, because their pI values are similar to each other. This also strongly suggests that CO-bound cyt c_3 is still biologically active and can work like cyt c_7 does. The microscopic redox potentials of cyt c_7 at the last reduction step were reported to be −201, −200, and −142 mV for hemes 1, 3, and 4 (according to the numbering in cyt c_3), respectively (*19*), which are higher than those of cyt c_3. Since the redox potentials would change upon CO binding, electron transport partners of CO-bound cyt c_3 can be different from those of intact cyt c_3. In fact, the activity of [NiFe]hydrogenase is inhibited by CO (*20*), although this is the major hydrogenase in the periplasm of a *Dv*MF cell and is thought to be a major electron transport partner of cyt c_3. Therefore, CO-bound cyt c_3 would have to receive electrons from other proteins, if it is inactivated.

It was reported that *D. vulgaris* can grow on CO, using it as a sole electron donor (*11*). Recently, CO cycling was reported to occur in *D. vulgaris* Hildenborough (*Dv*H) in association with H_2 cycling (*21*). A mutant with inactivated [Fe]hydrogenase accumulated a significant amount of CO. [Fe]Hydrogenase is the major hydrogenase in *Dv*H periplasm. There were three stages in the CO accumulation. At first, CO accumulates during the consumption of SO_4^{2-}. Namely, sulfate respiration is at work in this stage. Then, a burst of H_2 accumulation occurs without SO_4^{2-} consumption. In the last stage, the levels of both CO and H_2 are diminished with the recovery of SO_4^{2-} consumption. This result shows that the electron transport system in *D. vulgaris* is working in the presence of CO and in the absence of [Fe]hydrogenase, suggesting the presence of a CO-tolerant hydrogenase in the periplasm. Formation of CO-bound cyt c_3 would support the maintenance of sulfate respiration by introduction of alternative electron transport pathways. After the synthesis of new proteins for CO utilization through the activation of transcription of those genes by CO, sulfate respiration starts working again. Since *Dv*H is close to *Dv*MF in terms of the degree of sequence homology (88%) and energy metabolism (*1*), CO cycling would also occur in *Dv*MF.

In *Rhodospirillum rubrum*, CooA, a CO sensor protein, is activated by CO to initiate the transcription of the CO-related genes *cooMKLXUHF* (*10*). They have also been identified in the *Dv*H genome sequence, suggesting that the machinery found in *R. rubrum* is also operating in *D. vulgaris* cells (*22*). This kind of response usually takes some time, which could be the reason for retardation in the recovery of growth in *D. vulgaris* in the presence of CO. Nonetheless, the cells have to maintain their basic energy metabolism to survive even under such conditions. Since binding of CO to

cyt c_3 can induce an instantaneous change in the function of cyt c_3, it would work as an efficient backup to secure the energy metabolism in response to the appearance of risky CO. This is a kind of security system for an abrupt change in the circumstances of a living cell. The maximum amount of CO accumulated during CO cycling in *D. vulgaris* was ~8000 ppm in the gas phase (*21*), which corresponds to 7.6 μM in the aqueous solution. Since the K_d for the single-site binding of CO to cyt c_3 was 8.0 μM and the CO binding was reversible under the single-site binding condition, cyt c_3 can work as a CO-sensing security device in the electron transport pathway upon accumulation of CO. CO became toxic for sulfate-reducing bacteria at more than 4.5% CO in the gas phase (*11*, *23*). This corresponds to >42 μM CO in the aqueous phase, which induces binding of a second CO to cyt c_3 as can be seen in Figure 1B which presumably became biologically inactive because of its structural changes (Figure 2).

The CO utilization in *D. vulgaris* mentioned above strongly suggests that cyt c_3 is working as a bioactive CO sensor protein. Since cyt c_3 can bind a single CO molecule specifically and reversibly with a typical K_d for a CO sensor protein and can conduct redox reactions, cyt c_3 is a putative CO-sensing electron transport switcher. This is a novel type of CO sensor protein in comparison with CooA, NPAS2, and sGC in terms of its structure and function (*8*, *10*, *24*). CO sensor proteins reported so far have two structural units such as two domains or two subunits. In contrast, cyt c_3 apparently has just one domain. The tetraheme architecture plays the role of the multiunit structure for regulation of its function, and heme 2 assumes the regulatory unit. Although CooA and NPAS2 are involved in the regulation of transcription, cyt c_3 may be involved in that of energy transduction.

ACKNOWLEDGMENT

We are grateful to Dr. Erisa Harada (Institute for Protein Research, Osaka University) for her help and fruitful discussions about the experiments and to Prof. Michael F. Brown (University of Arizona, Tucson, AZ) for his valuable discussions about the manuscript.

SUPPORTING INFORMATION AVAILABLE

Amount of CO-bound cytochrome c_3 as a function of CO concentration in NMR experiments (Figure S1) and imide signals of the axial histidines in $^1H-^{15}N$ HSQC spectra of partially oxidized cytochrome c_3 forms in the presence of CO (Figure S2). This material is available free of charge via the Internet at http://pubs.acs.org.

REFERENCES

1. Odom, J. M., and Singleton, R., Jr., Eds. (1993) *The Sulfate-Reducing Bacteria: Contemporary Perspectives*, Springer-Verlag, New York.
2. Ambler, R. P. (1980) in *From Cyclotrons to Cytochromes* (Robinson, A. B., and Kaplan, N. O., Eds.) pp 263−279, Academic Press, London.
3. Harada, E., Fukuoka, Y., Ohmura, T., Fukunishi, A., Kawai, G., Fujiwara, T., and Akutsu, H. (2002) Redox-coupled conformational alterations in cytochrome c_3 from *D. vulgaris* Miyazaki F on the basis of its reduced solution structure, *J. Mol. Biol. 319*, 767−778.
4. Fan, K., Akutsu, H., Kyogoku, Y., and Niki, K. (1990) Estimation of microscopic redox potentials of a tetraheme protein, cytochrome c_3 of *Desulfovibrio vulgaris*, Miyazaki F, and partial assignments of heme groups, *Biochemistry 29*, 2257−2263.
5. Park, J.-S., Ohmura, T., Kano, K., Sagara, T., Niki, K., Kyogoku, Y., and Akutsu, H. (1996) Regulation of the redox order of four hemes by pH in cytochrome c_3 from *Desulfovibrio vulgaris* Miyazaki F, *Biochim. Biophys. Acta 1293*, 45−54.
6. Yagi, T., and Maruyama, K. (1971) Purification and properties of cytochrome c_3 of *Desulfovibrio vulgaris*, Miyazaki, *Biochim. Biophys. Acta 243*, 214−224.
7. O'Connor, D. B., Goldbeck, R. A., Hazzard, J. H., Kliger, D. S., and Cusanovich, M. A. (1993) Time-resolved absorption and magnetic circular dichroism spectroscopy of cytochrome c_3 from *Desulfovibrio*, *Biophys. J. 65*, 1718−1726.
8. Verma, A., Hirsch, D. J., Glatt, C. E., Ronnett, G. V., and Snyder, S. H. (1993) Carbon monoxide: A putative neural messenger, *Science 259*, 381−384.
9. Ryter, S. W., Morse, D., and Choi, A. M. K. (2004) Carbon monoxide: To boldly go where NO has gone before, *Science STKE 230*, re6.
10. Aono, S. (2003) Biochemical and biophysical properties of the CO-sensing transcriptional activator CooA, *Acc. Chem. Res. 36*, 825−831.
11. Lupton, F. S., Conrad, R., and Zeikus, J. G. (1984) Physiological function of hydrogen metabolism during growth of sulfidogenic bacteria on organic substrates, *FEMS Microbiol. Lett. 23*, 263−268.
12. Ozawa, K., Yasukawa, F., Fujiwara, Y., and Akutsu, H. (2001) A simple, rapid, and highly efficient gene expression system for multiheme cytochrome *c*, *Biosci., Biotechnol., Biochem. 65*, 185−189.
13. Ozawa, K., Takayama, Y., Yasukawa, F., Ohmura, T., Cusanovich, M. A., Tomimoto, Y., Ogata, H., Higuchi, Y., and Akutsu, H. (2003) Role of the aromatic ring of Tyr43 in tetraheme cytochrome c_3 from *Desulfovibrio vulgaris* Miyazaki F, *Biophys. J. 85*, 3367−3374.
14. Takayama, Y., Harada, E., Kobayashi, R., Ozawa, K., and Akutsu, H. (2004) Roles of noncoordinated aromatic residues in redox regulation of cytochrome c_3 from *Desulfovibrio vulgaris* Miyazaki F, *Biochemistry 43*, 10859−10866.
15. Yamashita, T., Hoashi, Y., Watanabe, K., Tomisugi, Y., Ishikawa, Y., and Uno, T. (2004) Roles of heme axial ligands in the regulation of CO binding to CooA, *J. Biol. Chem. 279*, 21394−21400.
16. Moon, R. B., and Richards, J. H. (1974) Carbon-13 magnetic resonance studies of the binding of carbon monoxide to various hemoglobins, *Biochemistry 13*, 3437−3443.
17. Behere, D. V., Gonzalez-Vergara, E., and Goff, H. M. (1985) Comparison of heme environments and proximal ligands in peroxidases and other hemoproteins through carbon-13 nuclear magnetic resonance spectroscopy of carbon monoxide complexes, *Biochem. Biophys. Res. Commun. 131*, 607−613.
18. Czjzek, M., Arnoux, P., Haser, R., and Shepard, W. (2001) Structure of cytochrome c_7 from *Desulfuromonas acetoxidans* at 1.9 Å resolution, *Acta Crystallogr. D57*, 670−678.
19. Correia, I. J., Paquete, C. M., Louro, R. O., Catarino, T., Turner, D. L., and Xavier, A. V. (2002) Thermodynamic and kinetic characterization of trihaem cytochrome c_3 from *Desulfuromonas acetoxidans*, *Eur. J. Biochem. 269*, 5722−5730.
20. Ogata, H., Mizoguchi, Y., Mizuno, N., Miki, K., Adachi, S., Yasuoka, N., Yagi, T., Yamauchi, O., Hirota, S., and Higuchi, Y. (2002) Structural studies of the carbon monoxide complex of [NiFe] hydrogenase from *Desulfovibrio vulgaris* Miyazaki F: Suggestion for the initial activation site for dihydrogen, *J. Am. Chem. Soc. 124*, 11628−11635.
21. Voordouw, G. (2002) Carbon monoxide cycling by *Desulfovibrio vulgaris* Hildenborough, *J. Bacteriol. 184*, 5903−5911.
22. Heidelberg, J. F., et al. (2004) The genome sequence of the anaerobic, sulfate-reducing bacterium *Desulfovibrio vulgaris* Hildenborough, *Nat. Biotechnol. 32*, 554−559.
23. Davydova, M., Savirova, R., Vylegzhanina, N., and Tarasova, N. (2004) Carbon monoxide and oxidative stress in *Desulfovibrio desulfuricans* B-1388, *J. Biochem. Mol. Toxicol. 18*, 87−91.
24. Dioum, E. M., Rutter, J., Tuckerman, J. R., Gonzalez, G., Gilles-Gonzalez, M.-A., and McKnight, S. L. (2002) NPAS2: A gas-responsive transcription factor, *Science 298*, 2385−2387.
25. Guex, N., and Peitsch, M. C. (1996) Swiss-PDBViewer: A fast and easy-to-use PDB viewer for Macintosh and PC, *Protein Data Bank Quarterly Newsletter 77*, 7.

BI051867I